

β 2 glycoprotein I participates in phagocytosis of apoptotic neurons and in vascular injury in experimental brain stroke

Journal of Cerebral Blood Flow & Metabolism
2021, Vol. 41 (8) 2038–2053
© The Author(s) 2021



Article reuse guidelines:
sagepub.com/journals-permissions
DOI: 10.1177/0271678X20984551
journals.sagepub.com/home/jcbfm



Claudia Grossi^{1,*} , Carolina Artusi^{2,3,*}, PierLuigi Meroni¹,
Maria Orietta Borghi^{1,3} , Laura Neglia⁴, Paola Adele Lonati¹,
Marco Oggioni⁴, Francesco Tedesco¹,
Maria-Grazia De Simoni⁴ and Stefano Fumagalli⁴

Abstract

Beta-2 Glycoprotein I (β 2-GPI) is the main target of anti-phospholipid antibodies (aPL) in the autoimmune anti-phospholipid syndrome, characterized by increased risk of stroke. We here investigated the antibody independent role of β 2-GPI after ischemia/reperfusion, modeled *in vivo* by transient middle cerebral artery occlusion (tMCAo) in male C57Bl/6j mice; *in vitro* by subjecting immortalized human brain microvascular endothelial cells (ihBMEC) to 16 h hypoxia and 4 h re-oxygenation. *ApoH* (coding for β 2-GPI) was upregulated selectively in the liver at 48 h after tMCAo. At the same time β 2-GPI circulating levels increased. β 2-GPI was detectable in brain parenchyma and endothelium at all time points after tMCAo. Parenchymal β 2-GPI recognized apoptotic neurons (positive for annexin V, C3 and TUNEL) cleared by CD68+ brain macrophages. Hypoxic ihBMEC showed increased release of IL-6, over-expression of *thrombomodulin* and *IL-1 α* after re-oxygenation with β 2-GPI alone. β 2-GPI interacted with mannose-binding lectin in mouse plasma and ihBMEC medium, potentially involved in formation of thrombi. We show for the first time that brain ischemia triggers the hepatic production of β 2-GPI. β 2-GPI is present in the ischemic endothelium, enhancing vascular inflammation, and extravasates binding stressed neurons before their clearance by phagocytosis. Thus β 2-GPI may be a new mediator of brain injury following ischemic stroke.

Keywords

Brain ischemia, β 2 glycoprotein I, complement system, thromboinflammation, mannose-binding lectin

Received 5 August 2020; Revised 6 November 2020; Accepted 2 December 2020

Introduction

Inflammation after stroke is strictly connected to cellular or molecular mediators of thrombosis, thus rising secondary mechanisms of lesion expansion. These events are referred to as thromboinflammation,¹ whose mediators remain amply undisclosed.

We here started from the notion that stroke is the most common severe neurologic complication in the anti-phospholipid syndrome (APS), an autoimmune disease characterized by high circulating levels of auto-antibodies.² APS patients experience the formation of thrombi and obstetric complications.³ Notably, the brain circulation is one of the

¹Istituto Auxologico Italiano, IRCCS, Laboratory of Immuno-Rheumatology, Milan, Italy

²Rheumatology Department, ASST Gaetano Pini-CTO, Milan, Italy

³Department of Clinical Sciences and Community Health, University of Milan, Milan, Italy

⁴Istituto di Ricerche Farmacologiche Mario Negri IRCCS, Department of Neuroscience, Milan, Italy

*These authors contributed equally to the work.

Corresponding authors:

Stefano Fumagalli, Istituto di Ricerche Farmacologiche Mario Negri IRCCS, via Mario Negri 2, Milano 20156, Italy.
Email: stefano.fumagalli@marionegri.it

Claudia Grossi, Istituto Auxologico Italiano, via Giuseppe Zucchi 18, Cusano, Milanino 20095, Italy.
Email: clgrossi@gmail.com

compartment affected by arterial thrombosis in APS patients, thus suggesting the presence of brain-selective detrimental mechanisms in the syndrome. In line with this, other neurological symptoms, like cognitive abnormalities, chorea and epilepsy, are known in APS patients, thus implying a direct effect of the auto-antibodies on brain cells.⁴

The main molecular target of the auto-antibodies in APS is β 2 glycoprotein I (β 2-GPI), a protein released by liver and found in blood physiologically. β 2-GPI physiological role is still scarcely understood. β 2-GPI is a circulating protein, composed of five domains, present physiologically in a range of 50–400 μ g/mL.^{5,6} Age, smoking, dyslipidemia and chronic infections cause β 2-GPI increase in plasma.⁷ It has been hypothesized that openings of the blood-brain barrier (BBB) in response to an endothelial damage facilitates the brain entry of auto-antibodies and β 2-GPI. In the brain, β 2-GPI may then target neurons, astrocytes and endothelium.⁸ Even though β 2-GPI has been mainly studied as the target of auto-antibodies, a pathophysiological effect of β 2-GPI itself has been proposed,^{3,9} introducing and supporting the hypothesis that β 2-GPI bridges inflammation and coagulation in different diseased conditions.⁹ This could be relevant in the context of brain ischemia, a condition inducing BBB leakage and thus possibly β 2-GPI brain entry, even in the absence of aPL.

Exploiting its ability to bind anionic surfaces,¹⁰ β 2-GPI changes conformation from a globular form into an open one that completely exposes domain 1 (D1), able to interact with other proteins^{5,6} including complement components. β 2-GPI indeed belongs to the superfamily of complement regulatory proteins and complement activation products were reported in APS patients.¹¹ Moreover complement components were found to co-localize with β 2-GPI and IgG on the endothelium of an APS patient, an interaction potentially involved in the pathogenesis of the thrombotic event through complement activation.¹² Recent work reported that β 2-GPI interacts with mannose-binding lectin (MBL), a recognition molecule of the lectin pathway of complement activation.¹³ This interaction may be particularly relevant in the context of ischemic stroke, where MBL plays a key role in post-stroke vascular damage, affecting endothelial cell structure,¹⁴ functionality and inflammatory profile.^{15,16} Thus β 2-GPI interaction with the complement system may underpin vascular damage after stroke.

We therefore decided to investigate the involvement of β 2-GPI in stroke pathophysiology and the potential interactions with the complement system. We used a clinically relevant murine model of stroke and analyzed, at different time points after the ischemic onset, β 2-GPI in plasma and brain (using an antibody

designed for open β 2-GPI exposing D1¹⁷). To dissect specific vascular effects associated to β 2-GPI, we used an *in vitro* model of ischemia/reperfusion on human brain microvascular cells exposed to human purified β 2-GPI.

Methods

Full methods are available as Supplementary Information.

Focal cerebral ischemia

Project approved by the Italian Ministry of Health (authorization number 224/2016-PR). Male 9–11 week old, 26–28 g, mice C57Bl/6J WT were used. The study was conducted according to the IMPROVE guidelines.¹⁸ This report adheres to the ARRIVE guidelines (check list as supplementary). Transient middle cerebral artery occlusion (tMCAo) was induced with the filament model.^{19,20} Surgery-associated mortality rate was 7%. Sham-operated mice received identical anesthesia and surgery without artery occlusion.

Quantification of infarct size

Lesion size was quantified on cresyl-violet stained sections after edema correction.²¹

Real time RT-PCR

Total RNA was extracted from the frozen liver or cultured cells scraped from the plates after re-oxygenation, using the miRNeasy kit (Qiagen) and reverse-transcribed. Real-time RT-PCR was conducted using Power SYBR Green (Applied Biosystems) and relative gene expression determined with $\Delta\Delta$ Ct method. Primer sequences are detailed in Supplementary Information.

Quantification of total β 2-GPI in murine plasma samples or human serum

β 2-GPI was quantified in murine EDTA-plasma samples and in the human serum (Innovative Research), used for *in vitro* experiments, as reported.²² We coated plates with a rabbit polyclonal anti- β 2-GPI antibody (1:2000, Invitrogen). Murine EDTA-plasma at final dilution 1:4050 or human serum at final dilution 1:1350 were incubated 1 h at room temperature (RT) with a goat polyclonal anti- β 2-GPI antibody (1:500, OriGene). We used a rabbit anti-goat IgG AP conjugate (1:1000, Invitrogen) to detect the signal. A purified murine (kindly gifted by Flavio Allegri and colleagues) or human β 2-GPI were used for calibration/standard curve.

Immunofluorescence

Antibodies and their concentrations are detailed in Supplementary Information. Immunofluorescence was acquired three-dimensionally with a 40x objective using an IX81 microscope with a confocal scan unit FV500. Images were managed and elaborated with Imaris v.6 (Bitplane) and arranged with GIMP. β 2-GPI *in vitro* signal was acquired using a widefield fluorescent microscope over randomly selected fields of view with a 20 \times objective. Signal was quantified by ImageJ.¹⁴ For immunofluorescence on culture media, 0.5 μ L of medium were spotted on glasses for microscopy and fixed for 15 minutes with 4% paraformaldehyde prior to labeling. Cells and conglomerates were visualized using differential interference contrast (DIC) microscopy with Nomarsky method.

Structured illumination microscopy (SIM)

SIM on brain sections was done with a Nikon SIM system with a 100x 1.49 NA oil immersion objective, managed by NIS elements software. Tissues were imaged at laser excitation of 405 (for nuclei), 488 (for β 2-GPI), 561 (for MBL-C) and 640 nm (for IB4) with a 3D-SIM acquisition protocol. Fourteen-bit images sized 1024 \times 1024 pixels with a single pixel of 0.030 μ m were acquired in a gray level range of 0-4000 to exploit the linear range of the camera (iXon ultra DU-897U, Andor) and to avoid saturation. Raw and reconstructed images were verified by the SIMcheck ImageJ plugin.²³

Gene basal expression and microarray analysis

Brain basal expression of *ApoH* in *mus musculus* was obtained from the online RNA-seq database available at: <http://www.brainrnaseq.org/24>. Published microarray data were used to compare gene expression levels (normalized log₂ OD) in 3 h tMCAo and 24 h tMCAo vs. untreated WT mice (dataset number: GSE32529, published in^{24,25}) using GEO2R software (NCBI).

Tunel

Apoptotic cells were labeled by *in situ* cell death detection kit (Roche, Mannheim, Germany²¹). For brain sections, TUNEL was acquired at 20x by an Olympus BX-61 Virtual Stage microscope and TUNEL cells identified over the ischemic ipsi-lateral striatum with ImageJ.^{21,26} For culture media, 0.5 μ L of medium were spotted on glasses for microscopy and fixed for 15 minutes with 4% paraformaldehyde prior to TUNEL reaction. Acquisition was done by an Olympus FV500 confocal microscope. TUNEL was visualized by excitation at 540 nm. Cells and

conglomerates were visualized with the same excitation wavelength using differential interference contrast (DIC) microscopy with Nomarsky method. TUNEL negative control was done by omitting the enzyme during the reaction. TUNEL positive control was done by treating the samples with 1 μ g/mL DNase.

Lectin pathway activation assay

A functional lectin pathway activity assay was done using EDTA-plasma diluted 2.5% in barbital-buffered saline (BBS) incubated for 15' at 37° C on 10 μ g/mL mannan-coated plates.²⁷ C3 deposition was revealed using a polyclonal anti-human-C3c antibody (2.4 μ g/mL, Dako) and an alkaline-phosphatase labeled goat anti-rabbit IgG (1 μ g/mL, Sigma). Absorption at optical density (OD) 405 nm measured using Infinite M200 spectrofluorimeter (Tecan, CH).

Phagocytosis assessment

Co-localization was analyzed over 3-dimensional fields measuring 180 \times 135 \times 7 μ m, obtained by stacking 31 confocal planes at a 800 \times 600 pixels, distanced by a z-axis step of 0.23 μ m. Three-dimensional fields were positioned over the ischemic area using the motorized stage under the control of xy Stage software (Olympus). For each coronal section, 4 nonoverlapping fields, over a 2 \times 2 matrix were aligned. Quantification of double-positive voxels (co-localization) was performed with Imaris (Bitplane) using the ImarisColoc algorithm.²⁸ Signal intensity over a volume with no positive staining (background) was calculated for each channel and used as the lower signal threshold. Voxels that were over lower thresholds for both channels were co-localized. A colocalization channel (gray) containing only co-localized voxels was generated and visualized by surface rendering (IsoSurface; Imaris) using the thresholds applied for colocalization analysis. Co-localization is expressed as percentage of CD68/CD11b double-positive voxels over total CD11b-positive voxels.

Sandwich ELISA

EDTA-plasma was diluted 1.25%, culture media was diluted 1.25, 2.5, 5 and 10% in BBS and incubated for 1 h 30' at 37° C on plates coated overnight with a mini-body obtained from the B2 clone of the anti- β 2-GPI (MBB2, 0.06 μ g/mL, see supplementary information). Next plate was incubated 1 h 30' RT with anti-MBL-A, MBL-C or human MBL antibodies (1 μ g/mL, Hycult). Absorption was read at OD 450 nm using the Infinite M200 spectrofluorimeter (Tecan, CH).

In vitro model of ischemia/reperfusion

Immortalized human-derived microvascular endothelial cells (ihBMEC) were placed into a hypoxic chamber (Ruskin Invivo2 400) at 37°C, and maintained in deoxygenated culture medium at O₂ 0.5%, CO₂ 5% and N₂ 94.5% for 16 h.¹⁴ Next, cells underwent 4 h re-oxygenation exposed to 30% human serum (Innovative Research), 10 µg/mL rhMBL (R&D systems), 100 µg/mL human purified β2-GPI, or both rhMBL and β2-GPI diluted in culture medium.

β2-GPI preparation

Human β2-GPI was purified from a pool of 100 human aPL negative healthy donors serum samples checking aPL absence with ELISA.^{29,30} Cyanine5.5 fluolabelling of β2-GPI (β2-GPI^{cy.55}) was performed as previously described.²⁹ Endotoxin levels were evaluated performing Lymulus Amebocyte Lysate test, Pierce™ Chromogenic Endotoxin Quant Kit (Thermoscientific) on the final product of β2GPI purification.

IL-6 Medium dosage

Media from ihBMECs were collected after 4 h re-oxygenation and analyzed using the Quantikine® ELISA Human IL-6 Immunoassay (R&D systems) according to the manufacturer's instructions.

Statistical analysis

Mice were randomly allocated to surgery and assigned across cages and days. Wells for *in vitro* ischemia/reperfusion were randomly allocated to treatments. All analysis were done by blinded investigators. Group size was defined based on a pilot experiment assessing *ApoH* overexpression induced at 24 h after tMCAo, using the formula: $n = 2\sigma^2 f(\alpha, \beta) / \Delta^2$ (SD in groups = σ , type I error $\alpha = 0.05$, type II error $\beta = 0.2$, percentage difference between groups $\Delta = 200$, i.e. a two-time increase in *ApoH* expression than basal levels). The pilot experiment resulted in a standard deviation (SD) between groups of $\sigma = 23$, therefore yielding $n = 5$. Groups were compared by analysis of variance and *post hoc* test, as indicated in each figure legend. The parametric or non-parametric test was selected after a Kolmogorov-Smirnov test for normality. The constancy of variances was checked by Bartlett test and, if not satisfied, a Welch correction was used. Statistical analysis was done with the standard software package GraphPad Prism (GraphPad Software Inc., San Diego, CA, USA, version 7.0); *p* values lower than 0.05 were considered significant.

Results

The experiments followed the plan in Figure 1(a). The tMCAo induced by the filament model caused a clear lesion – indicated by a pale area after Cresyl violet staining – in the striatum and cortex ipsi-lateral to the lesion starting from 90' after the ischemic onset (ischemic volume was $10.16 \pm 2.87 \text{ mm}^3 \pm \text{SD}$). The lesion was fully developed at 24-48 h (57.17 ± 12.08 and $63.42 \pm 3.21 \text{ mm}^3$, respectively). At 7d the proper identification of the pale stained area is hampered by immune cell infiltration, therefore lower values for ischemic volume were quantified ($37.90 \pm 12.18 \text{ mm}^3$, Figure 1(b)).

Brain ischemia induced the up-regulation of *ApoH* – the gene coding for β2-GPI – in the liver at 24 and 48 h (2.17 ± 0.88 and 4.00 ± 2.53 fold-change than sham $\pm \text{SD}$, respectively, Figure 1(c)). In line with the time of maximal up-regulation of *ApoH* in the liver, circulating levels of β2-GPI increased at 48 h after tMCAo ($190.8 \pm 32.8 \text{ µg/mL}$, mean $\pm \text{SD}$) than sham ($141.3 \pm 6.6 \text{ µg/mL}$, Figure 1(d)). Notably, β2-GPI plasma levels decreased at 90' after tMCAo ($121.5 \pm 8.4 \text{ µg/mL}$) compared to sham, possibly as a result of circulating protein consumption, i.e. binding to its target.

Confocal microscopy revealed β2-GPI brain presence in areas pertinent to the ischemic territory, including the cortex, piriform cortex and striatum (Figure 1(e)). We here presented confocal images relative to the cortical ischemic territory. β2-GPI was present in the brain in a D1-exposing conformation (recognized by MBB2) starting from 90' after tMCAo and up to 7d, at variance with sham-operated mice (Figure 1(f)). β2-GPI was located in brain parenchyma and on brain vessels, as better depicted in the three-dimensional renderings. None of the brain populations is able to express the *ApoH* gene, according to single-cell RNA-seq transcriptomic databases (Figure 1(g)). Moreover, tMCAo did not induced *ApoH* upregulation in the brain (Figure 1(h)) or in the blood cells (Figure 1(i)), as shown by analysis of microarray databases, thus suggesting that β2-GPI of liver origin infiltrated in the brain through the damaged blood-brain barrier.

In the brain parenchyma, at all time points, β2-GPI co-localized with NeuN, a neuronal marker (Figure 2(a)), but not with glial fibrillary acidic protein (GFAP, astrocytes, Figure 2(b)), nor with CD11b (microglia/macrophages, Figure 2(c)). We observed that ramified CD11b+ cells, likely to be microglia due to their morphology, contacted β2-GPI (arrows in Figure 2(c)) suggesting an interaction between microglia and brain structures labeled by β2-GPI (endothelial cells and neurons).

Since β2-GPI has been reported to bind to apoptotic cells,¹⁰ we explored the temporal pattern of apoptosis

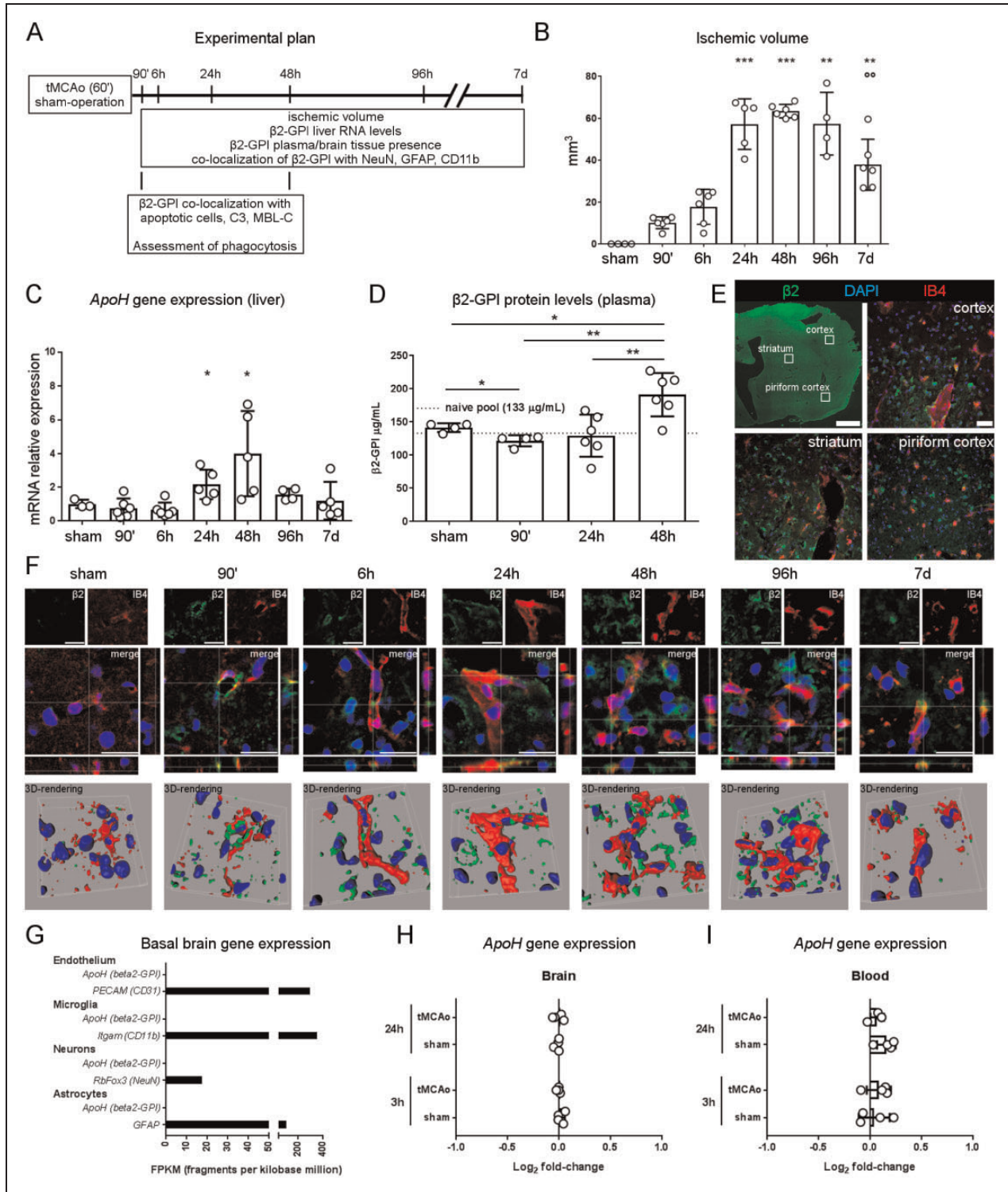


Figure 1. Experimental plan and time course of the ischemic volume and β2-GPI after brain ischemia. (a) Experimental plan. (b) The ischemic lesion was already seen at 90' after tMCAo and, as expected, reached its maximum at 48 h. At subsequent times the infiltration of glial cells into the lesioned area hampers proper lesion quantification through the identification of a pale cresyl violet stained area, therefore lower values for ischemic volume are quantified. Bars at mean and dot plots ± sd, n = 4–6. Normal distributions (Kolmogorov-Smirnoff test) with unequal variances (Bartlett test), Welch corrected t-test, $^{***}p < 0.01$, $^{***}p < 0.001$ vs. 90', $^{oo}p < 0.01$ vs. 48 h. (c) Ischemia induced the expression of β2-GPI in the liver at 24 h and 48 h after the insult. Bars at mean and dot plots ± sd, n = 4–6. Normal distributions (Kolmogorov-Smirnoff test) with unequal variances (Bartlett test), Welch corrected t-test, $^{*}p < 0.05$ vs. 90'. (d) The presence of circulating β2-GPI was measured in plasma from naïve, tMCAo or sham-operated mice.

(continued)

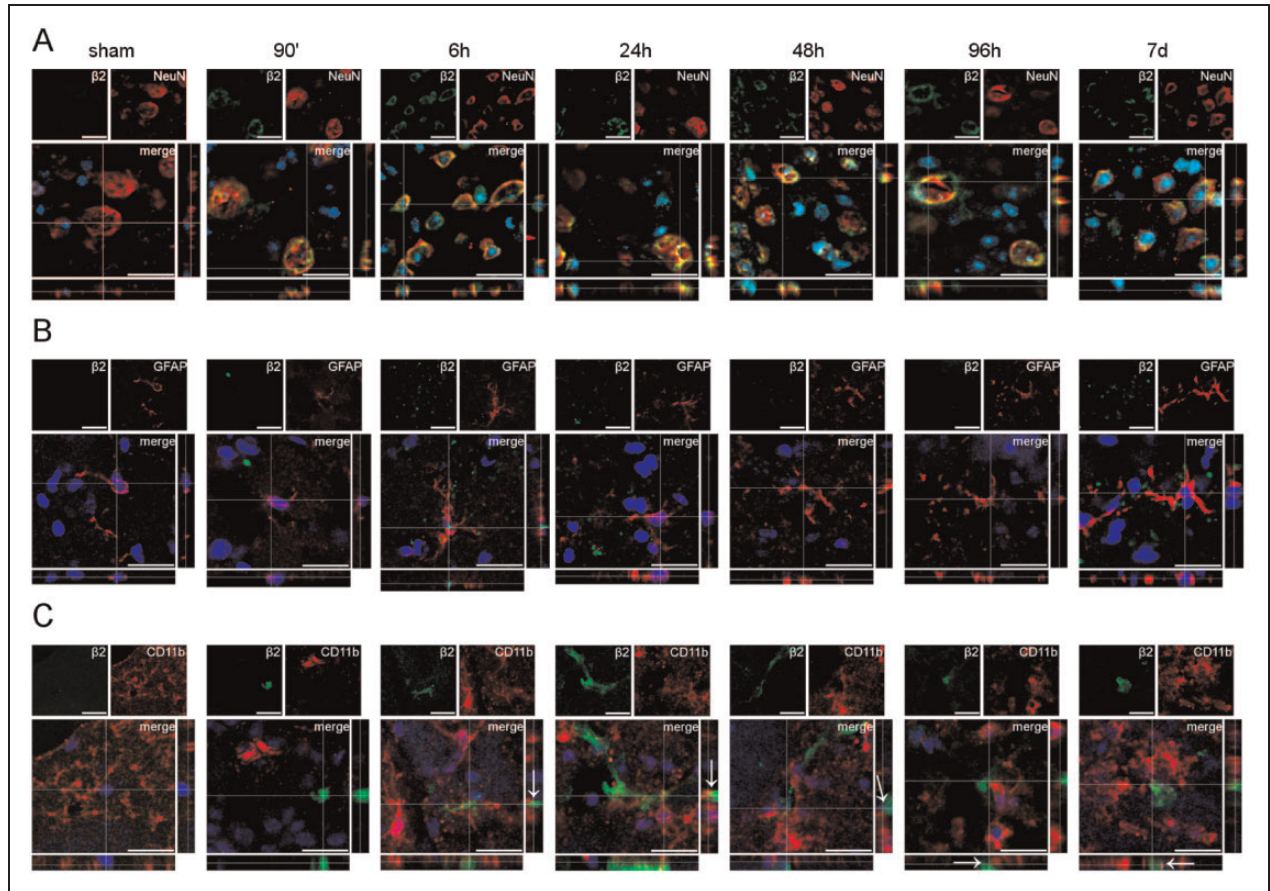


Figure 2. Co-localization of open β 2-GPI (green) with neurons (NeuN, red), astrocytes (GFAP, red) or microglia/macrophages (CD11b, red) in the cortical ischemic area. (a) β 2-GPI co-localized with neurons at all times analyzed, as shown by the xy single plane image with z-axis projections. (b) β 2-GPI was faintly present on astrocytes, with no co-localization observed. (c) β 2-GPI did not co-localize with microglia/macrophages. Notably, some CD11b+ cell ramifications took contact with β 2-GPI positive structures (arrows in z projections in c). Nuclei are in blue. Images are representative of at least three independent experiments. Scale bars = 20 μ m.

in our model by staining terminal apoptotic cells by TUNEL.³¹ Sparse apoptotic cells appeared as early as 90' after tMCAo (12.2 ± 8.3 cells/mm² \pm SD), reaching their maximal density in the ischemic territory at 48 h (719.6 ± 471.8 cells/mm², Figure 3(a) and (b)). As previously reported by our group and others,^{16,32} the lectin

pathway of complement activation is a major inflammatory event following tMCAo, and produces downstream effects comprising opsonization of apoptotic cells to drive their clearance.³³ In line with TUNEL+ cell presence, using a functional mannan assay detecting C3b deposition due to MBL,³⁴ we observed

Figure 1. Continued

Circulating levels of β 2-GPI increased significantly at 48 h after tMCAo. Bars at mean and dot plots \pm sd, n = 4–6. Normal distributions (Kolmogorov-Smirnoff test) with unequal variances (Bartlett test), Welch corrected t-test, * $p < 0.05$, ** $p < 0.01$. (e) A MBB2 antibody able to bind the open form of β 2-GPI was used to label β 2-GPI in the brain tissue. β 2-GPI was seen in brain areas pertinent to the ischemic territory at 48 h after tMCAo. (f) Sham-operated mice showed a very weak positivity for open β 2-GPI (green), while at all times after tMCAo open β 2-GPI was present both in brain parenchyma and on the cerebral endothelium (IB4, red) in regions within the ischemic territory. The three-dimensional renderings clearly show the presence of open β 2-GPI on brain vessels. Nuclei are in blue. Images are representative of at least three independent experiments. Scale bars = 20 μ m. (g) Basal gene expression (fragments per kilobase million, FPKM) of *ApoH* (coding for β 2-GPI) in *mus musculus* brain cell populations. Endothelial cells (expressing *PECAM*), microglia (expressing *Itgam*), neurons (expressing *RbFox3*) and astrocytes (expressing *GFAP*) do not express *ApoH*. Data obtained from single cell RNA-seq databases as described in methods. (h, i) Expression changes (microarray analysis) in brain ischemic cortex (h) and blood cells (i) for *ApoH* following tMCAo, showing no induction of its expression at 3 h or 24 h after the ischemic onset. Bars at mean and dot plots \pm sd, n = 4. Data expressed as Log₂-fold change than untreated mice, two-way ANOVA followed by Sidak's post hoc test, not statistically significant. Data obtained from microarray databases as described in methods.

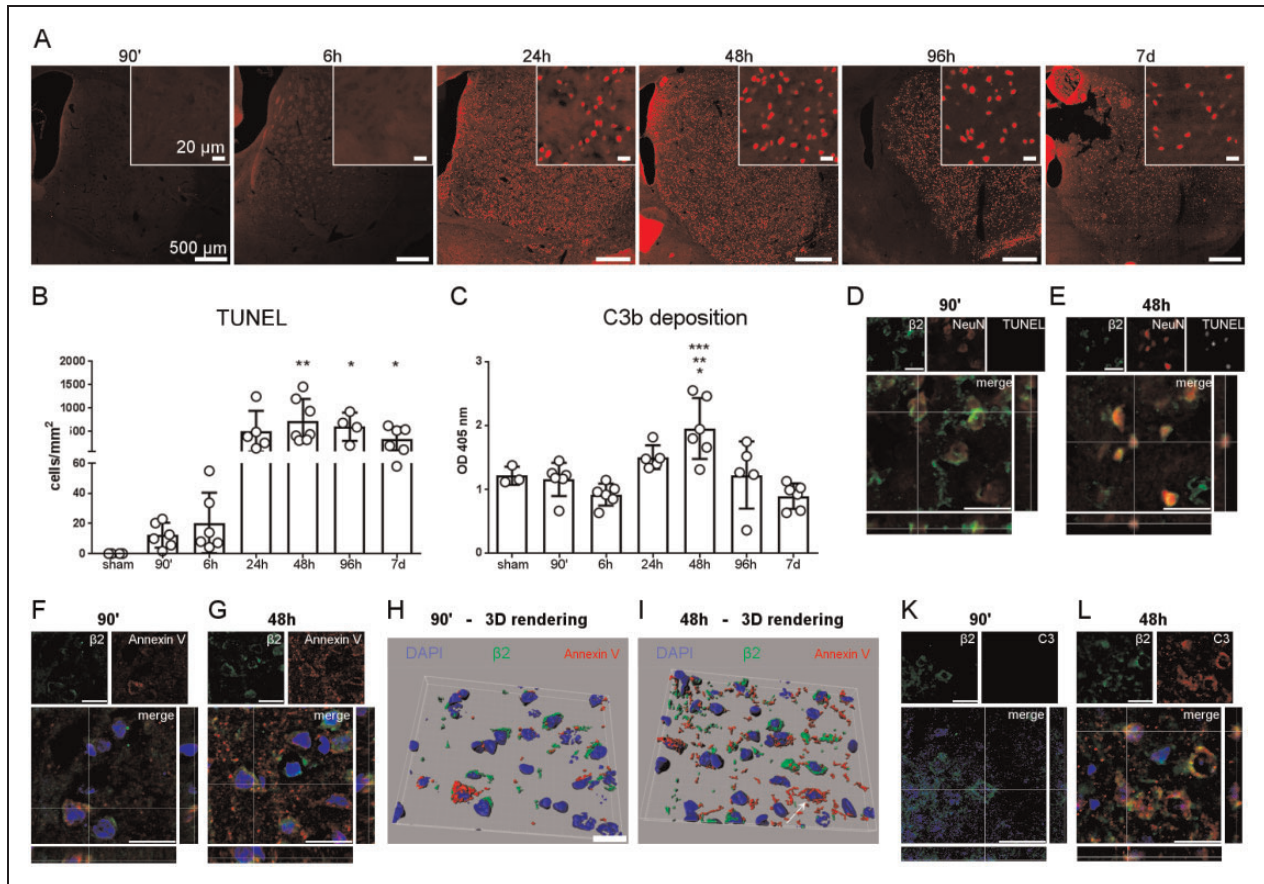


Figure 3. Time course of apoptosis and activation of the complement system after the ischemic onset and co-localization of open β 2-GPI (green) with apoptotic neurons (NeuN/TUNEL), annexin V (red) or C3 (red) in the cortical ischemic area. (a) Terminal apoptotic cells (TUNEL positive, red) are visible starting from 90' after ischemia until 7d. Scale bars = 500 μ m or 20 μ m (inserts). (b) Quantification of TUNEL Positive cells in the ischemic area. Bars at mean and dot plots \pm sd, n = 4-6. Normal distributions (Kolmogorov-Smirnoff test) with unequal variances (Bartlett test), Welch corrected t-test, $^{**}p < 0.01$, $^{*}p < 0.05$ vs. 90'. (c) The lectin pathway of complement activation, a major driver of opsonization of apoptotic cells, peaks at 48 h after the ischemic onset. Bars at mean and dot plots \pm sd, n = 3 (sham) - 6. One-way ANOVA followed by Tukey's post hoc test, $^{*}p < 0.05$ vs. sham and 4d, $^{**}p < 0.01$ vs. 90' and $^{***}p < 0.001$ vs. 6h and 7d. (d, e) 90' and 48h after ischemia were chosen as reference time points showing presence of β 2-GPI (green) on neurons (NeuN, red) which were not apoptotic (90', d) or terminally apoptotic (48h, TUNEL, white, e). (f-i) At both 90' (f) and 48h (g) after tMCAo β 2-GPI co-localized with cells positive for annexin V (red), an early marker of apoptosis. Three-dimensional renderings showed that all β 2-GPI positive cells expressed annexin V (h, i). Few cells appeared annexin V positive and β 2-GPI negative (arrow, i). Scale bar = 20 μ m. (k) At 90' after tMCAo β 2-GPI (green) was present within the ischemic territory, while C3 was not detectable. (l) At 48h C3 (red) was present in the ischemic area and co-localized with β 2-GPI. Images are representative of at least three independent experiments. Scale bars = 20 μ m.

maximal C3b deposition at 48 h after tMCAo (Figure 3 (c)). We therefore selected 48 h as a reference time point and compared it with 90' after tMCAo, when apoptosis was in its early phases.

Co-localization studies between β 2-GPI, NeuN and TUNEL showed terminally apoptotic neurons, visible at 48 h, positive for β 2-GPI (Figure 3(d) and (e)). Annexin V, an early marker of apoptosis, co-localized with β 2-GPI at 90' after tMCAo (Figure 3(f) and (g)). Three-dimensional renderings showed that all β 2-GPI positive cells expressed annexin V, while few annexin V positive cells did not show β 2-GPI positivity (Figure 3

(h) and (i)). This observation might imply that β 2-GPI recognizes cells already undertaking the apoptotic fate. C3 brain deposition was observed at 48 h and co-localized with β 2-GPI (Figure 3(k) and (l)). In order to explore whether β 2-GPI represents an early marker of dying cells undergoing clearance by phagocytosis, we analyzed the phagocytic activity of brain myeloid cells at 90' and 48h. The co-localization of CD11b (membrane myeloid cell marker) and CD68 (lysosomal marker), indicative of membrane proximity of lysosomes and therefore of active particle internalization,^{28,35} was higher at 48 h (Manders' coefficient

22.79 ± 3.62% ± SD) than 90' (13.53 ± 2.10%, Figure 4 (a) to (c)). At 48 h, neurons displaying β 2-GPI were enveloped by myeloid cells highly positive for CD68 (Figure 4(d) and (d')), suggesting the involvement of β 2-GPI in neuronal clearance after ischemia.

The high glycosylation profile of β 2-GPI suggests a possible interaction with recognition molecules of the complement system. In the ischemic stroke scenario the interaction of β 2-GPI with mannose-binding lectin (MBL) could be critical. Indeed MBL is a recognition molecule of the complement system that deposits on the ischemic endothelium causing post-stroke vascular dysfunction.¹⁶ We thus evaluated β 2-GPI:MBL interaction *in vivo* by confocal microscopy. At 48 h after tMCAo β 2-GPI and MBL-C - the murine isoform present at higher levels at this time point³⁴ - showed a weak co-localization although

present on the same vessel (Figure 5(a)). In order to rule out that co-localized pixels depended on the resolution limit of confocal microscopy, we analyzed brain sections by superresolved structured illumination microscopy (SIM, Figure 5(b)). SIM revealed that most of β 2-GPI and MBL-C signals did not co-localize, and that signal overlapping was rare (arrow in Figure 5(b)). Imaging data suggest therefore that the two proteins mostly do not interact on the ischemic vessels *in vivo*. However, when β 2-GPI:MBL interaction was assessed *ex vivo* using plasma from mice, a biphasic interaction between β 2-GPI and MBL-C was observed at 90' and 4d after tMCAo (respectively 1.80 ± 0.06 and 1.93 ± 0.48 fold-change than sham, mean ± SD, Figure 5(c)). At variance, β 2-GPI did not interact with the MBL-A murine isoform (Figure 5(c)).

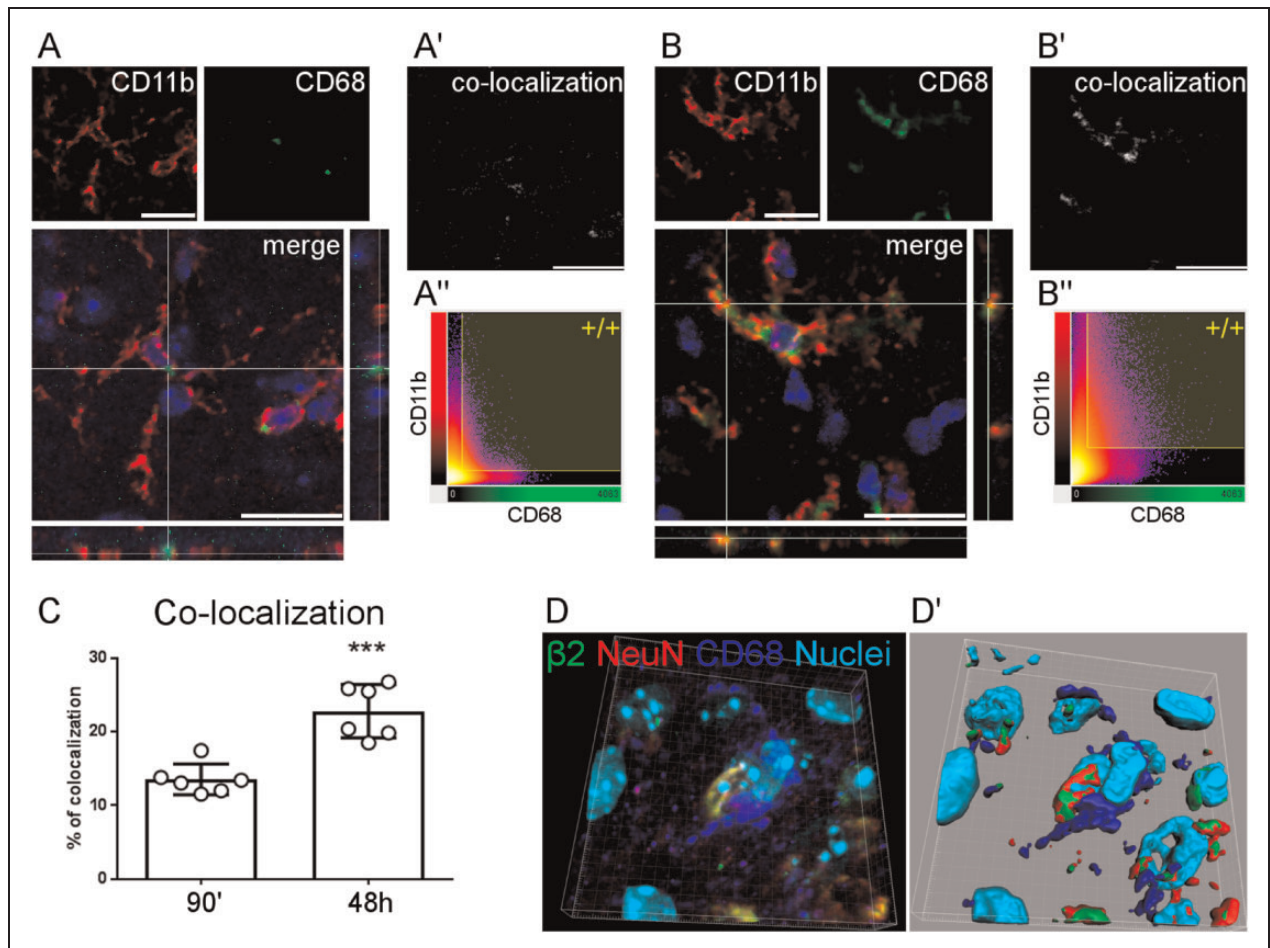


Figure 4. Assessment of the phagocytic phenotype by immunofluorescence for CD11b (red) and CD68 (green) at 90' and 48 h after tMCAo. (a–a'') At 90' CD11b positive cells showed low co-localization with CD68. (b–b'') At 48 h, when the apoptotic process was clearly seen in the ischemic brain, CD11b co-localized significantly with CD68. Nuclei are in blue. Scale bars = 20 μ m. (c) The double positive pixels (up-right quadrant in a' and b'') were higher at 48 h than 90', indicating an increased phagocytic phenotype of brain myeloid cells at 48 h. Bars at mean and dot plots \pm sd, n = 6. Normal distributions (Kolmogorov-Smirnoff test), t-test, *** p < 0.001 vs. 90'. (d, d') Three-dimensional image and its rendering showing at 48 h a phagocytic cell (CD68, dark blue) engulfing a neuron (NeuN, red) tagged by β 2-GPI (green), suggesting the involvement of β 2-GPI in neuronal clearance after tMCAo.

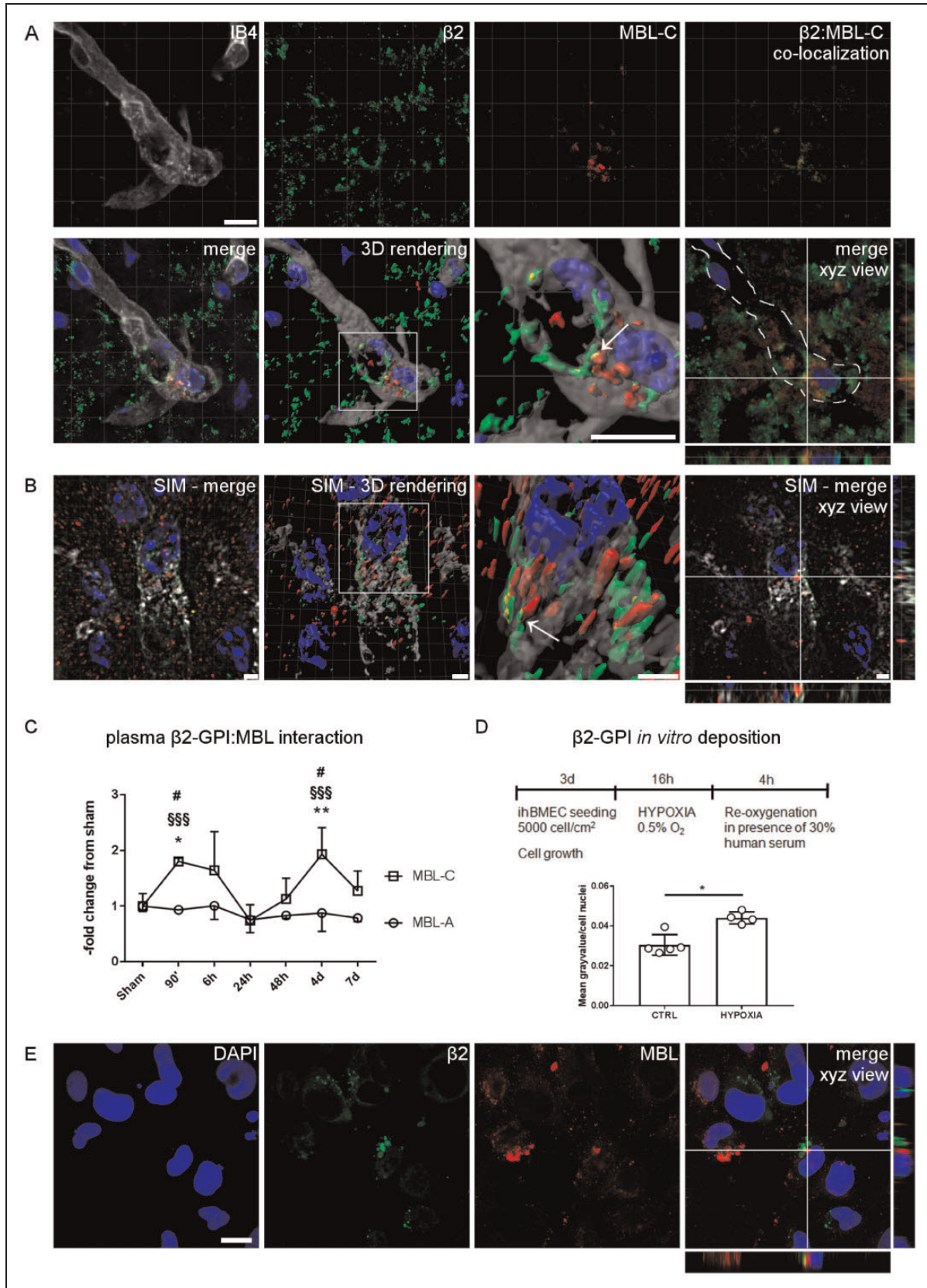


Figure 5. Analysis of β 2-GPI interaction with mannose-binding lectin (MBL). (a) Vessels pertinent to the ischemic territory at 48 h (IB4, white; outline traced in the merge panel) showed presence of both β 2-GPI (green) and MBL (MBL-C murine isoform, red).

(continued)

We next used an *in vitro* model of ischemia/reperfusion on ihBMEC. We performed hypoxia (0.5% oxygen) for 16 h and re-oxygenated ihBMEC in presence of 30% human serum (Figure 5(d)), according to a protocol reported to induce MBL deposition and cell death.¹⁴ After re-oxygenation, β 2-GPI deposition increased on hypoxic than normoxic (control) cells (0.044 ± 0.003 vs. 0.030 ± 0.005 mean gray value/cell number, mean \pm SD, Figure 5(d)). In line with *in vivo* observations β 2-GPI and MBL did not co-localize, even when present on the same ihBMEC (Figure 5(e)).

We exposed hypoxic or normoxic ihBMEC to 30% human serum, human-purified β 2-GPI, human recombinant MBL or both proteins (Figure 6(a)). We assessed the content of β 2-GPI in the human serum, that resulted in a mean \pm SD concentration of 300 ± 86 μ g/mL, thus 90 μ g/mL when the serum was applied at 30% dilution on ihBMEC. Endotoxins were checked for each preparation by a LAL test, resulting <0.10 Endotoxin Unit (EU) per 1 μ g of proteins. We firstly defined the working concentration of human-purified β 2-GPI by a dose-response study. Since we aimed at identifying the pro-inflammatory response driven by β 2-GPI, we dosed the release of IL-6 in culture media after re-oxygenation of ihBMEC with 5, 10, 50, 100 or 200 μ g/mL of β 2-GPI. As a positive control, ihBMEC exposed to high IL-1 β concentrations (50000 pg/mL) showed strong release of IL-6 in both normoxic (415.5 ± 110.2 pg/mL \pm SD) and hypoxic (717.0 ± 68.2) conditions. Hypoxic ihBMEC released significantly higher amount of IL-6 starting from a concentration of β 2-GPI of 100 μ g/mL (21.5 ± 4.66 pg/mL \pm SD) compared to normoxic cells (5.3 ± 1.5 , Figure 6 (b)). Considering that the baseline concentration of mouse circulating β 2-GPI was similar (see Figure 1 (d)) as well as that of 30% human serum, we thus decided to expose ihBMEC to 100 μ g/mL of human-purified β 2-GPI for next experiments.

Either normoxic or hypoxic ihBMEC re-oxygenated in presence of both β 2-GPI and MBL showed floating insoluble bodies, removed after medium collection (Figure 6(c)). At variance with this, when

re-oxygenation was done in presence of β 2-GPI or MBL alone, no floating insoluble bodies were observed (Supplementary Figure 1). We pooled the collected media and incubated them in a sandwich ELISA using MBB2-coated plates and the anti-MBL antibody as revealing reagent. Media obtained from hypoxic ihBMEC exposed to both β 2-GPI and MBL showed β 2-GPI:MBL interaction (Figure 6(d)). In order to explore whether the insoluble bodies after re-oxygenation with β 2-GPI and MBL contained apoptotic cells, we plated the media on glasses for microscopy and run TUNEL. In either normoxic or hypoxic conditions few apoptotic cells were found in conglomerates seen by differential interference contrast (DIC) microscopy (Figure 6(e), negative controls in Supplementary Figure 2). The conglomerates showed also a positive signal for β 2-GPI, suggesting its ability to target apoptotic cells (Figure 6(e'), negative controls in Supplementary Figure 3).

ihBMEC re-oxygenated with β 2-GPI and/or MBL showed decreased cell viability compared to vehicle-exposed cells, either after normoxia or hypoxia (Supplementary Figure 4). MBL alone further decreased ihBMEC viability in hypoxic vs. normoxic cells (5435.7 ± 1072.7 vs. 11491.0 ± 3612.7 Alamar Blue fluorescence \pm SD), in line with its direct toxic effects on the ischemic endothelium.¹⁴ β 2-GPI alone did not further affect cell viability after hypoxia, while it did so when present with MBL either after normoxia (5454.9 ± 1978.5) or hypoxia (5565.9 ± 2146.4 , Supplementary Figure 4). We next analyzed IL-6 released in culture media. Basal levels of IL-6 in serum were 5 pg/mL. As a positive control, ihBMEC exposed to high IL-1 β concentrations (50000 pg/mL) showed strong release of IL-6 in both normoxic (246.5 ± 10.6 pg/mL \pm SD) and hypoxic (604.0 ± 15.6) conditions. IL-6 increased after hypoxia and re-oxygenation with 30% human serum compared to normoxic control (44.8 ± 4.2 vs. 18.5 ± 5.9 , pg/mL \pm SD), similarly after re-oxygenation with β 2-GPI (46.8 ± 14.4 vs. 24.0 ± 7.1) and, at lower extent, with β 2-GPI and MBL (23.3 ± 7.9 vs. 8.5 ± 1.9 , Figure 6(f)). Notably

Figure 5. Continued

The two proteins showed weak co-localization at confocal microscopy. Nuclei are in blue. Scale bar = 10 μ m. (b) Superresolution by structured illumination microscopy (SIM) showed that β 2-GPI and MBL-C mostly did not co-localize, presenting very rare overlapping of signals (arrow). Scale bars = 2 μ m. (c) Plasma interaction between β 2-GPI and MBL murine isoforms (MBL-A and MBL-C) was assessed by a sandwich ELISA, using plates coated with MBB2. While no interaction was observed with MBL-A at all time points, β 2-GPI interacted with MBL-C in a biphasic manner, peaking at 90' and 4d after tMCAo. Points at mean \pm sd, n = 4–6. Two way ANOVA followed by Tukey's post hoc test, * $p < 0.05$, ** $p < 0.01$ vs. sham MBL-C; §§§ $p < 0.001$ vs. 24 h MBL-C, # $p < 0.05$ vs. 48 h MBL-C. (d) Experimental plan for *in vitro* ischemia/reperfusion model on cultured immortalized human-derived microvascular endothelial cells (ihBMEC). After 4 h of re-oxygenation in presence of 30% human serum, hypoxic cells had increased presence of β 2-GPI. Bars at mean and dot plots \pm sd, n = 4–5. Normal distribution (Kolmogorov-Smirnoff test), t-test, * $p < 0.05$. (e) Confocal image showing ihBMEC after re-oxygenation with 30% human serum. Although observed on the same cell, β 2-GPI (green) and MBL (red) did not co-localized, as clearly shown on the orthogonal projections. Nuclei are in blue. Scale bar = 20 μ m.

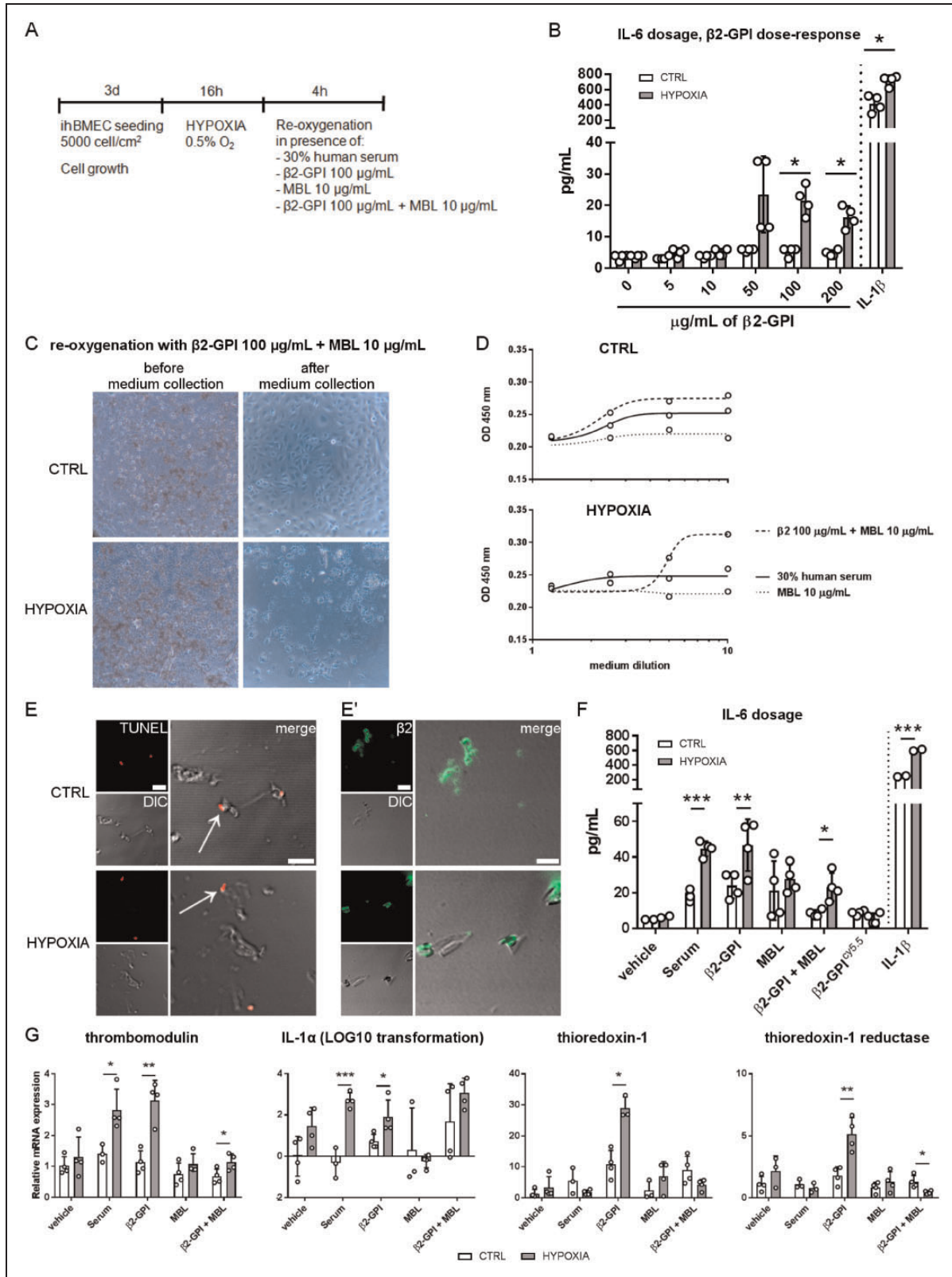


Figure 6. Effects of exposure of ihBMEC to serum, β2-GPI, MBL or both β2-GPI and MBL during 4h re-oxygenation. (a) Experimental plan for in vitro ischemia/reperfusion model on cultured ihBMEC. Human purified β2-GPI and recombinant human MBL were used. (b) Human purified β2-GPI dose-response experiment. Starting from a dose of 100 μg/mL, β2-GPI caused an increased release of IL-6 by hypoxic compared to normoxic ihBMEC. Exposure to 50000 pg/mL of IL-1β was used as the experimental positive

(continued)

fluolabeled $\beta 2$ -GPI^{cy5.5} did not induce the same effect than bare $\beta 2$ -GPI.

We next analyzed gene expression of *thrombomodulin* and *IL-1 α* - markers associated with a vascular inflammatory profile after brain ischemia¹⁶ - in re-oxygenated ihBMEC. Re-oxygenation in presence of 30% human serum, $\beta 2$ -GPI or both $\beta 2$ -GPI and MBL induced the over-expression of *thrombomodulin* (respectively 2.82 ± 0.68 , 3.14 ± 0.64 or 1.15 ± 0.27 fold-change than CTRL vehicle, mean \pm SD, Figure 6 (g)). Re-oxygenation in presence of 30% human serum or $\beta 2$ -GPI induced the over-expression of *IL-1 α* (respectively 2.71 ± 0.36 or 1.91 ± 0.81 , Figure 6(g)). As $\beta 2$ -GPI alone induced a vascular inflammatory profile, we analyzed the expression of genes controlling protein red-ox state, a critical feature of $\beta 2$ -GPI immunogenicity and physiological functions.^{36,37} Both *thioredoxin-1* and *thioredoxin-1 reductase* were selectively up-regulated in hypoxic ihBMEC exposed to $\beta 2$ -GPI (28.93 ± 3.64 and 5.12 ± 1.34 , fold-change than CTRL vehicle, mean \pm SD, Figure 6(g)).

Discussion

The present study reports for the first time that: 1) brain ischemia triggers the hepatic production of $\beta 2$ -GPI; 2) $\beta 2$ -GPI deposits on the ischemic endothelium and extravasates in the parenchyma as early as 90' after the ischemic onset; 3) $\beta 2$ -GPI tags stressed neurons and participates, in association with the complement system, to their clearing through phagocytosis; 4) $\beta 2$ -GPI alone induces damage to the ischemic endothelium. As such, we propose $\beta 2$ -GPI as a new mediator of brain injury after ischemic stroke.

Most of what is known about $\beta 2$ -GPI regards its role in APS, a clinical condition characterized by formation of thrombi, where $\beta 2$ -GPI is a target of aPL. APS patients experience different neurological complications, among which stroke represents the most frequent event (5.3%) followed by transient ischemic

attack as the second-most frequent (4.7%) event, per report.³⁸ Moreover APS is the most common cause of stroke in young adults - less than 45 years-old.³⁹ Besides the targeting of the cerebral circulation, a direct effect of $\beta 2$ -GPI on brain resident populations has been suggested, but never demonstrated directly.

Our ischemia/reperfusion murine model induced the overexpression of *ApoH* gene (coding for $\beta 2$ -GPI) in the liver and increased $\beta 2$ -GPI circulating levels at 48 h after ischemic onset. Whether *ApoH* overexpression depended on specific transcription factors stimulated by post-stroke inflammation needs to be explored. We hypothesize that *ApoH* overexpression was a feedback response to the usage of the circulating protein after ischemia - as suggested by the decrease of $\beta 2$ -GPI circulating levels at 90' after tMCAo compared to sham - inducing its liver production. In line with circulating protein usage, we detected $\beta 2$ -GPI on the ischemic endothelium as well as in the brain parenchyma, starting from 90' - a time point when the ischemic vessel leakage is already in place⁴⁰ - and lasting till 7d after the ischemic onset. Brain cells do not express *ApoH*, nor do blood cells, thus all brain parenchymal $\beta 2$ -GPI had liver origin. At 90' after tMCAo brain parenchymal $\beta 2$ -GPI localized on early apoptotic neurons exposing phosphatidylserine - recognized by annexin V - bearing a negative charge. Literature reports that anionic surfaces are among the possible targets of $\beta 2$ -GPI, exploiting the positive charges located on its domain 5 (D5). On binding to negatively charged epitopes - such as phosphatidylserine - $\beta 2$ -GPI exposes completely the D1 domain, which may be normally hidden.^{6,41,42} We here show that $\beta 2$ -GPI linked to apoptotic neurons' exposed phosphatidylserine, visualized by annexin V staining. This binding induced the exposure of D1, visualized using the minibody specifically designed for $\beta 2$ -GPI D1. At 48 h after tMCAo, terminal apoptotic neurons - positive for TUNEL assay - were still recognized by open (D1

Figure 6. Continued

control. Bars at mean and dot plots \pm sd, n = 4 wells. Multiple t-tests, *p < 0.05. (c) Brightfield images showing the presence of insoluble bodies after re-oxygenation of normoxic or hypoxic ihBMEC with both $\beta 2$ -GPI and MBL. These insoluble bodies were not seen in the well after medium collection for further analysis. (d) Culture media collected after re-oxygenation were analyzed with a sandwich ELISA coating the plates with MBB2. Hypoxic ihBMEC exposed to both $\beta 2$ -GPI and MBL showed increased interaction between the two proteins than normoxic cells (CTRL) or those exposed to 30% human serum or MBL alone. (e, e') Culture media after re-oxygenation with $\beta 2$ -GPI and MBL was spotted on glasses for microscopy. TUNEL showed few apoptotic cells (red) within conglomerates (visualized by differential interference contrast, DIC) seen in either control or hypoxic cells (arrows, e). Immunofluorescence using MBB2 showed the presence of $\beta 2$ -GPI (green) associated with the conglomerates in both conditions (e'). Scale bars = 10 μ m. (f) IL-6 was dosed on the collected media. IL-6 levels increased in hypoxic ihBMEC exposed to 30% human serum, $\beta 2$ -GPI or $\beta 2$ -GPI + MBL compared to CTRL. Bars at mean and dot plots \pm sd, n = 3-4 wells. Multiple t-tests, **p < 0.01, ***p < 0.001. (g) Real time RT-PCR measuring inflammatory gene expression in ihBMEC after re-oxygenation. *Thrombomodulin* was over-expressed in hypoxic ihBMEC after 30% human serum, $\beta 2$ -GPI or $\beta 2$ -GPI + MBL. *IL-1 α* was over-expressed in hypoxic ihBMEC after 30% human serum or $\beta 2$ -GPI. *Thioredoxin-1* and *thioredoxin-1 reductase* were over-expressed selectively in hypoxic ihBMEC exposed to $\beta 2$ -GPI. Bars at mean and dot plots \pm sd, n = 3-4 wells. Multiple t-tests, *p < 0.05, **p < 0.01, ***p < 0.001.

exposing) β 2-GPI. At this time, open β 2-GPI co-localized also with complement C3 - an opsonin required for cell clearance through phagocytosis - in line with β 2-GPI function as a complement regulator.⁴³ The antibody used to localize C3 does not distinguish the native from the cleaved form so that we cannot conclude that β 2-GPI co-localized with activated C3. We previously showed that the presence of C3 in the brain increases after tMCAo, but is not seen in mice deficient for MASP-2, the main serine protease associated to lectin pathway activation.⁴⁴ Moreover MASP-2 deficient mice are neuroprotected from brain ischemia, lending support that C3 present in the brain is implicated in neuronal damage. While the functional relationship between β 2-GPI and C3 deposited on neurons is not clear, the early detection of β 2-GPI on stressed neurons suggests that this protein may be considered an early marker of damaged neurons before C3 deposition and eventual clearance.

β 2-GPI D1 can bind low density lipoprotein receptors present on macrophage membrane, an event facilitating the engulfment of β 2-GPI-phosphatidylserine and β 2-GPI-apoptotic cell complexes.¹⁰ At 48 h we observed that β 2-GPI positive neurons were recognized and surrounded by tissue macrophages highly positive for CD68, a lysosomal marker,⁴⁵ committed to active phagocytosis, thus suggesting a β 2-GPI involvement in neuronal clearing after brain ischemia.

Data *in vivo* showed that β 2-GPI also targets brain ischemic vessels, implying its potential role in stroke secondary thromboinflammatory mechanisms. Blood-borne cascades like coagulation, contact/kinin, and complement system act on the ischemic vascular compartment⁴⁶ and contribute to stroke pathogenesis, as reported in experimental models¹⁶ and humans.⁴⁷ We previously reported in the same murine model of stroke used here, that thromboinflammatory mechanisms driving post-stroke vascular damage are coordinated by mannose-binding lectin (MBL), a recognition molecule starting the lectin pathway of the complement system.^{14,16} MBL recognizes highly glycosylated proteins, making β 2-GPI a putative target. In line with this, MBL was recently reported to bind β 2-GPI *in vitro*, although independently of β 2-GPI glycosylation.¹³ We here analyzed their interaction on the ischemic vessels by immunofluorescence. We focused on the 48 h time point, when the ischemic lesion is fully developed and β 2-GPI as well as MBL-C - the MBL murine isoform with similar carbohydrate specificity than the human protein^{48,49} - are seen on ischemic vessels (shown here and in²⁰). β 2-GPI and MBL-C showed a very weak co-localization, even when found on the same vessel. Superresolved microscopy by SIM identified few overlapping voxels between the two signals. Thus a molecular interaction between β 2-GPI and

MBL - which was previously shown on the femoral artery of an APS patient¹³ - cannot be ruled out. However our data suggest that the two proteins have very rare interactions on the brain ischemic vessel luminal surface. At variance we detected a clear-cut fluid phase β 2-GPI interaction with MBL-C, but not with MBL-A, in tMCAo mice plasma. β 2-GPI and MBL-C interacted biphasically, possibly due to plasma protein availability resulting from a net balance between the consumed (used for target binding) and synthesized (produced by the liver) proteins. Their interaction was indeed observed as early as 90', when constitutive protein levels may be still sufficient, and at 4d after ischemia, following the peak of liver gene expression for both molecules (at 48 h, reported here and in³⁴). Notably in the sandwich ELISA we trapped (caught) β 2-GPI on MBB2-coated plates and revealed the MBL isoforms with appropriate antibodies. The finding that MBL-C interacts with β 2-GPI indicates that brain ischemia offered activatory stimuli favoring their interaction, which was not observed in plasma from non-ischemic mice. We also propose that MBL-C binding to β 2-GPI did not use its D1. This latter hypothesis has been formulated based on the fact that the D1 was still available to MBB2 binding in the sandwich ELISA, and parallels recent findings showing that MBL binds preferentially D2 and D4 of β 2-GPI, in a glycosylation independent manner.¹³

Comparing MBL murine isoforms, MBL-C is the less efficient complement activator, moreover its usage following ischemia is delayed than MBL-A. Nevertheless MBL-C has a detrimental role in stroke pathophysiology,³⁴ lending support to its implication in secondary thromboinflammatory mechanisms, that likely involve its interaction with β 2-GPI.

The apparent discrepancy between fluid-phase and tissue β 2-GPI:MBL interaction might depend on different reasons, namely 1) the analyzed time points: in the first hours after tMCAo MBL has been reported to act mainly in circulation, where it binds platelets inducing their inflammatory profile.¹⁶ 2) β 2-GPI:MBL interaction occurs selectively in thrombi. If this is the case, we could be unable to detect the small clots in brain microvessels after tMCAo,⁵⁰ because they were washed during the perfusion fixation procedure to sacrifice the mice. 3) That the sandwich ELISA caused the formation of β 2-GPI:MBL complexes in the well.

To dissect the vascular effects of β 2-GPI we used an *in vitro* model of ischemia/reperfusion on cultured microvascular cells of human origin (ihBMEC¹⁴). β 2-GPI and MBL deposition was seen on ischemic ihBMEC, with no co-localization. A fluid phase β 2-GPI:MBL interaction was seen in culture medium from ischemic ihBMEC after 4h re-oxygenation in presence of the two proteins. The *in vitro* model

therefore mirrored what observed *in vivo*. Interestingly the presence of both β 2-GPI and MBL during re-oxygenation was associated to the formation of insoluble bodies in the culture medium. This event was seen either in normoxic or hypoxic ihBMEC and possibly contributed to cell death in both conditions. Insoluble bodies contained few apoptotic cells, thus offering a target for β 2-GPI that was indeed visualized on insoluble bodies by immunofluorescence.

We next analyzed the vascular response to ischemia/reperfusion in presence of β 2-GPI and/or MBL in terms of IL-6 release. IL-6 has a pleiotropic role in inflammation,⁵¹ including the induction of acute phase protein such as MBL,⁵² and is a key proinflammatory mediator in stroke⁵³ acting in a self-amplifying network upon its release by brain resident cells.⁵⁴ Moreover IL-6 has been proposed like a modulator of aPL-mediated activation of endothelial cells.⁵⁵ Nevertheless, β 2-GPI in the absence of aPL was shown to modulate serum levels of IL-6 when administered intravenously to healthy mice.⁵⁶ We here report that hypoxic ihBMEC re-oxygenated in presence of human serum had increased IL-6 release in culture medium. We also measured a clear IL-6 release in hypoxic ihBMEC re-oxygenated in presence of β 2-GPI alone, suggesting that β 2-GPI could induce an early pro-inflammatory milieu on the endothelium after stroke. Interestingly we observed lower IL-6 release in the hypoxic medium when β 2-GPI was co-incubated with MBL, supporting the idea that MBL could bind and thus retain in the fluid phase part of β 2-GPI. The lower IL-6 release by ihBMEC re-oxygenated with both β 2-GPI and MBL may also be due to the presence of fewer cells in the well compared to other conditions. In fact we observed decreased ihBMEC viability after re-oxygenation with both β 2-GPI and MBL in normoxic and hypoxic cells.

Hypoxic ihBMEC re-oxygenated with human serum also up-regulated *thrombomodulin* and *IL-1 α* , two markers whose up-regulation is associated with stroke-induced vascular inflammation.^{57–59} Similarly to what observed for IL-6 release, β 2-GPI alone induced *thrombomodulin* and *IL-1 α* up-regulation in hypoxic ihBMEC, lending further support to β 2-GPI ability to induce a vascular inflammatory profile.

We noticed that fluolabelled β 2-GPI^{Cy5.5} did not induce the same pro-inflammatory effects than bare β 2-GPI. As a possible explanation, we hypothesized that the Cy5.5 tag influenced the ability of β 2-GPI to switch its red-ox state and thus affected β 2-GPI immunogenicity and functions.^{36,37} The expression of *thioredoxin-1* and *thioredoxin-1 reductase* in hypoxic ihBMEC was up-regulated after re-oxygenation with bare β 2-GPI, suggesting that the red-ox state of the protein may be a key feature in β 2-GPI role after

stroke. We did not observe the same gene up-regulations when β 2-GPI was co-incubated with MBL, lending further support to MBL's ability to bind and possibly retain in the fluid phase part of β 2-GPI.

In conclusion our data points at β 2-GPI like a mediator of injury in the ischemic brain. While the pathogenic role of β 2-GPI and its potential interaction with MBL need to be clarified, its presence on stressed brain structures (e.g. apoptotic neurons and ischemic vessels) demonstrates β 2-GPI's ability to target the brain, thus explaining why neurological complications are common in APS patients. Moreover, having identified for the first time a β 2-GPI involvement in stroke even in absence of auto-antibodies, our work provides new insights into the protein pathophysiological role and makes β 2-GPI a new candidate therapeutic target deserving further investigations.

Data availability

Raw data are available at a Figshare repository, doi: 10.6084/m9.figshare.1,22,64,677.

Funding

The author(s) disclosed receipt of the following financial support for the research, authorship, and/or publication of this article: This work was funded by Fondazione Cariplo, Ricerca Biomedica condotta da Giovani Ricercatori, Grant 2015-1003.

Declaration of conflicting interests

The author(s) declared no potential conflicts of interest with respect to the research, authorship, and/or publication of this article.

Authors' contributions

CG, CA, SF planned and did the experiments, analyzed the data and drafted the ms; LN, PAL, MO, MOB did the experiments and analyzed the data; PLM, FT, MGDS planned the experiments and critically reviewed the ms.

Supplemental material

Supplemental material for this article is available online.

ORCID iDs

Claudia Grossi  <https://orcid.org/0000-0003-0811-2472>
Maria Orietta Borghi  <https://orcid.org/0000-0001-8967-9678>
Maria-Grazia De Simoni  <https://orcid.org/0000-0002-0259-0003>

Acknowledgements

The authors thank Thomas McDonnell and Maria Gabriella Raimondo for their valuable technical advice on β 2-GPI plasma dosage, and Nicola Pozzi for manuscript revision.

References

1. De Meyer SF, Denorme F, Langhauser F, et al. Thromboinflammation in stroke brain damage. *Stroke* 2016; 47: 1165–1172.
2. Cervera R. Antiphospholipid syndrome. *Thromb Res* 2017; 151(Suppl 1): S43–S47.
3. Meroni PL, Borghi MO, Grossi C, et al. Obstetric and vascular antiphospholipid syndrome: same antibodies but different diseases? *Nat Rev Rheumatol* 2018; 14: 433–440.
4. Miyakis S, Lockshin MD, Atsumi T, et al. International consensus statement on an update of the classification criteria for definite antiphospholipid syndrome (APS). *J Thromb Haemost* 2006; 4: 295–306.
5. de Laat B and de Groot PG. Autoantibodies directed against domain I of beta2-glycoprotein I. *Curr Rheumatol Rep* 2011; 13: 70–76.
6. de Groot PG and Meijers JCM. $\beta(2)$ -Glycoprotein I: evolution, structure and function. *J Thromb Haemost JTH* 2011; 9: 1275–1284.
7. Meroni PL, Gerosa M, Raschi E, et al. Updating on the pathogenic mechanisms 5 of the antiphospholipid antibodies-associated pregnancy loss. *Clin Rev Allergy Immunol* 2008; 34: 332–337.
8. Carecchio M, Cantello R and Comi C. Revisiting the molecular mechanism of neurological manifestations in antiphospholipid syndrome: beyond vascular damage. *J Immunol Res* 2014; 2014: 239398.
9. McDonnell T, Wincup C, Buchholz I, et al. The role of beta-2-glycoprotein I in health and disease associating structure with function: more than just APS. *Blood Rev* 2020; 39: 100610.
10. Maiti SN, Balasubramanian K, Ramoth JA, et al. Beta-2-glycoprotein I-dependent macrophage uptake of apoptotic cells. Binding to lipoprotein receptor-related protein receptor family members. *J Biol Chem* 2008; 283: 3761–3766.
11. Lonati PA, Scavone M, Gerosa M, et al. Blood Cell-Bound C4d as a marker of complement activation in patients with the antiphospholipid syndrome. *Front Immunol* 2019; 10: 773.
12. Meroni PL, Macor P, Durigutto P, et al. Complement activation in antiphospholipid syndrome and its inhibition to prevent rethrombosis after arterial surgery. *Blood* 2016; 127: 365–367.
13. Durigutto P, Macor P, Pozzi N, et al. Complement activation and thrombin generation by MBL bound to β 2-Glycoprotein I. *J Immunol* 2020; 205: 1385–1392.
14. Neglia L, Fumagalli S, Orsini F, et al. Mannose-binding lectin has a direct deleterious effect on ischemic brain microvascular endothelial cells. *J Cereb Blood Flow Metab* 2020; 40: 1608–1620.
15. de la Rosa X, Cervera A, Kristoffersen AK, et al. Mannose-binding lectin promotes local microvascular thrombosis after transient brain ischemia in mice. *Stroke* 2014; 45: 1453–1459.
16. Orsini F, Fumagalli S, Császár E, et al. Mannose-Binding lectin drives platelet inflammatory phenotype and vascular damage after cerebral ischemia in mice via IL (interleukin)-1 α . *Arterioscler Thromb Vasc Biol* 2018; 38: 2678–2690.
17. Agostinis C, Durigutto P, Sblattero D, et al. A non-complement-fixing antibody to β 2 glycoprotein I as a novel therapy for antiphospholipid syndrome. *Blood* 2014; 123: 3478–3487.
18. Percie Du Sert N, Alfieri A, Allan SM, et al. The IMPROVE guidelines (ischaemia models: procedural refinements of in vivo experiments). *J Cereb Blood Flow Metab* 2017; 37: 3488–3517.
19. De Simoni MG, Rossi E, Storini C, et al. The powerful neuroprotective action of C1-inhibitor on brain ischemia-reperfusion injury does not require C1q. *Am J Pathol* 2004; 164: 1857–1863.
20. Orsini F, Villa P, Parrella S, et al. Targeting mannose binding lectin confers long lasting protection with a surprisingly wide therapeutic window in cerebral ischemia. *Circulation* 2012; 126: 1484–1494.
21. Perego C, Fumagalli S and De Simoni M-G. Temporal pattern of expression and colocalization of microglia/macrophage phenotype markers following brain ischemic injury in mice. *J Neuroinflammation* 2011; 8: 174.
22. Ioannou Y, Zhang J-Y, Qi M, et al. Novel assays of thrombogenic pathogenicity in the antiphospholipid syndrome based on the detection of molecular oxidative modification of the major autoantigen β 2-glycoprotein I. *Arthritis Rheum* 2011; 63: 2774–2782.
23. Ball G, Demmerle J, Kaufmann R, et al. SIMcheck: a toolbox for successful super-resolution structured illumination microscopy. *Sci Rep* 2015; 5: 15915.
24. Zhang Y, Chen K, Sloan SA, et al. An RNA-sequencing transcriptome and splicing database of glia, neurons, and vascular cells of the cerebral cortex. *J Neurosci* 2014; 34: 11929–11947.
25. Stevens SL, Leung PY, Vartanian KB, et al. Multiple preconditioning paradigms converge on interferon regulatory factor-dependent signaling to promote tolerance to ischemic brain injury. *J Neurosci* 2011; 31: 8456–8463.
26. Schindelin J, Arganda-Carreras I, Frise E, et al. Fiji: an open-source platform for biological-image analysis. *Nat Methods* 2012; 9: 676–682.
27. Fumagalli S, Perego C, Zangari R, et al. Lectin pathway of complement activation is associated with vulnerability of atherosclerotic plaques. *Front Immunol* 2017; 8: 288.
28. Zanier ER, Pischiutta F, Riganti L, et al. Bone marrow mesenchymal stromal cells drive protective M2 microglia polarization after brain trauma. *Neurotherapeutics* 2014; 11: 679–695.
29. Agostinis C, Biffi S, Garrovo C, et al. In vivo distribution of β 2 glycoprotein I under various pathophysiologic conditions. *Blood* 2011; 118: 4231–4238.
30. Andreoli L, Chighizola CB, Nalli C, et al. Clinical characterization of antiphospholipid syndrome by detection of IgG antibodies against β 2-glycoprotein I domain I and domain 4/5: ratio of anti-domain I to anti-domain 4/5 as a useful new biomarker for antiphospholipid syndrome. *Arthritis Rheumatol* 2015; 67: 2196–2204.
31. Zanier ER, Marchesi F, Ortolano F, et al. Fractalkine receptor deficiency is associated with early protection but

- late worsening of outcome following brain trauma in mice. *J Neurotrauma* 2016; 33: 1060.
32. Cervera A, Planas AM, Justicia C, et al. Genetically-defined deficiency of mannose-binding lectin is associated with protection after experimental stroke in mice and outcome in human stroke. *PLoS One* 2010; 5: e8433.
 33. Orsini F, De Blasio D, Zangari R, et al. Versatility of the complement system in neuroinflammation, neurodegeneration and brain homeostasis. *Front Cell Neurosci* 2014; 8: 380.
 34. Neglia L, Oggioni M, Mercurio D, et al. Specific contribution of mannose-binding lectin murine isoforms to brain ischemia/reperfusion injury. *Cell Mol Immunol* 2020; 17: 218–226.
 35. Fumagalli S, Fiordaliso F, Perego C, et al. The phagocytic state of brain myeloid cells after ischemia revealed by superresolution structured illumination microscopy. *J Neuroinflammation* 2019; 16: 9.
 36. Raimondo MG, Pericleous C, Radziszewska A, et al. Oxidation of β_2 -glycoprotein I associates with IgG antibodies to domain I in patients with antiphospholipid syndrome. *PLoS One* 2017; 12: e0186513.
 37. Ioannou Y, Zhang J-Y, Passam FH, et al. Naturally occurring free thiols within beta 2-glycoprotein I in vivo: nitrosylation, redox modification by endothelial cells, and regulation of oxidative stress-induced cell injury. *Blood* 2010; 116: 1961–1970.
 38. Cervera R, Piette J-C, Font J, et al. Antiphospholipid syndrome: clinical and immunologic manifestations and patterns of disease expression in a cohort of 1,000 patients. *Arthritis Rheum* 2002; 46: 1019–1027.
 39. Cervera R, Serrano R, Pons-Estel GJ, et al. Morbidity and mortality in the antiphospholipid syndrome during a 10-year period: a multicentre prospective study of 1000 patients. *Ann Rheum Dis* 2015; 74: 1011–1018.
 40. Fumagalli S, Ortolano F and De Simoni M-G. A close look at brain dynamics: cells and vessels seen by in vivo two-photon microscopy. *Prog Neurobiol* 2014; 121: 36–54.
 41. Miyakis S, Giannakopoulos B and Krilis SA. Beta 2 glycoprotein I—function in health and disease. *Thromb Res* 2004; 114: 335–346.
 42. de Laat B, van Berkel M, Urbanus RT, et al. Immune responses against domain I of β_2 -glycoprotein I are driven by conformational changes: domain I of β_2 -glycoprotein I harbors a cryptic immunogenic epitope. *Arthritis Rheum* 2011; 63: 3960–3968.
 43. Gropp K, Weber N, Reuter M, et al. β_2 -glycoprotein I, the major target in antiphospholipid syndrome, is a special human complement regulator. *Blood* 2011; 118: 2774–2783.
 44. Orsini F, Chrysanthou E, Dudler T, et al. Mannan binding lectin-associated serine protease-2 (MASP-2) critically contributes to post-ischemic brain injury independent of MASP-1. *J Neuroinflammation* 2016; 13: 213.
 45. Fumagalli S, Perego C, Pischiutta F, et al. The ischemic environment drives microglia and macrophage function. *Front Neurol* 2015; 6: 81.
 46. Fumagalli S and De Simoni M-G. Lectin complement pathway and its bloody interactions in brain ischemia. *Stroke* 2016; 47: 3067–3073.
 47. Arsava EM, Arat A, Topcuoglu MA, et al. Angiographic microcirculatory obstructions distal to occlusion signify poor outcome after endovascular treatment for acute ischemic stroke. *Transl Stroke Res* 2018; 9: 44–50.
 48. Hansen S, Thiel S, Willis A, et al. Purification and characterization of two mannan-binding lectins from mouse serum. *J Immunol* 2000; 164: 2610–2618.
 49. Sastry R, Wang JS, Brown DC, et al. Characterization of murine mannose-binding protein genes Mbl1 and Mbl2 reveals features common to other collectin genes. *Mamm Genome* 1995; 6: 103–110.
 50. del Zoppo GJ and Mabuchi T. Cerebral microvessel responses to focal ischemia. *J Cereb Blood Flow Metab* 2003; 23: 879–894.
 51. Turner MD, Nedjai B, Hurst T, et al. Cytokines and chemokines: at the crossroads of cell signalling and inflammatory disease. *Biochim Biophys Acta* 2014; 1843: 2563–2582.
 52. Antony JS, Ojurongbe O, Meyer CG, et al. Correlation of interleukin-6 levels and lectins during schistosoma haematobium infection. *Cytokine* 2015; 76: 152–155.
 53. Erta M, Quintana A and Hidalgo J. Interleukin-6, a major cytokine in the Central nervous system. *Int J Biol Sci* 2012; 8: 1254–1266.
 54. Gertz K, Kronenberg G, Kälin RE, et al. Essential role of interleukin-6 in post-stroke angiogenesis. *Brain* 2012; 135: 1964–1980.
 55. Vega-Ostertag M, Casper K, Swerlick R, et al. Involvement of p38 MAPK in the up-regulation of tissue factor on endothelial cells by antiphospholipid antibodies. *Arthritis Rheum* 2005; 52: 1545–1554.
 56. Zhou S, Lu M, Zhao J, et al. The purification of reduced β_2 -glycoprotein I showed its native activity in vitro. *Lipids Health Dis* 2017; 16: 173.
 57. Dharmasaroja P, Dharmasaroja PA and Sobhon P. Increased plasma soluble thrombomodulin levels in cardioembolic stroke. *Clin Appl Thromb Hemost* 2012; 18: 289–293.
 58. Kuo C-H, Chen P-K, Chang B-I, et al. The recombinant lectin-like domain of thrombomodulin inhibits angiogenesis through interaction with Lewis Y antigen. *Blood* 2012; 119: 1302–1313.
 59. Wong R, Lénárt N, Hill L, et al. Interleukin-1 mediates ischaemic brain injury via distinct actions on endothelial cells and cholinergic neurons. *Brain Behav Immun* 2019; 76: 126–138.